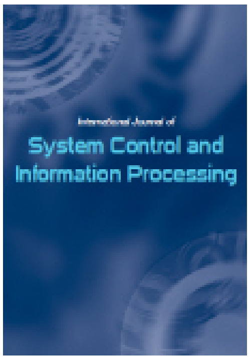

International Journal of System Control and Information Processing

ISSN online: 1759-9342 - ISSN print: 1759-9334
https://www.inderscience.com/ijscip

Integration of sensing, communication, and control for UAV-assisted data transmission in industrial IoT systems

Qirui Luo, Ling Lyu, Yanpeng Dai

DOI: 10.1504/IJSCIP.2024.10066317

Article History:

Received:	22 July 2023
Last revised:	25 July 2023
Accepted:	26 March 2024
Published online:	27 June 2025

Integration of sensing, communication, and control for UAV-assisted data transmission in industrial IoT systems

Qirui Luo, Ling Lyu* and Yanpeng Dai

School of Information Science and Technology,
Dalian Maritime University,
Dalian, 116026, China
Email: luoqirui@dlmu.edu.cn
Email: linglyu@dlmu.edu.cn
Email: yanpengdai@dlmu.edu.cn
*Corresponding author

Abstract: With the development of unmanned system, unmanned aerial vehicles (UAVs) and automated guided vehicles (AGVs) are widely used in industrial filed to assist the monitoring data transmission. However, the mobility of UAVs and AGVs make it challenging to timely obtain the accurate channel condition. In order to address this issue, this paper firstly proposed a sensing-communication-control integrated architecture for UAV-assisted industrial Internet of Things (IoT) systems. Then, the integration of sensing, communication and control (ISCC) scheme is investigated to improve the data transmission rate. Moreover, a ratio of transmission rate to power consumption maximisation problem is formulated to maximise the overall performance. As the formulated problem includes a rank-one constraint, a dual-layer penalty based successive convex approximation algorithm is designed to effectively solve the non-convex optimisation problem. Finally, simulation results verify the effectiveness and superiority of the proposed ISCC scheme in improving the overall performance of UAV-assisted industrial IoT systems.

Keywords: ISAC; integrated sensing and communication; UAV-assisted data transmission; unmanned aerial vehicle; industrial IoT; IoT; Internet of Things; non-convex problem; dual-layer penalty; SCA; successive convex approximation.

Reference to this paper should be made as follows: Luo, Q., Lyu, L. and Dai, Y. (2025) 'Integration of sensing, communication, and control for UAV-assisted data transmission in industrial IoT systems', *Int. J. System Control and Information Processing*, Vol. 4, No. 3, pp.220–234.

Biographical notes: Qirui Luo received the Bachelor's degree from Henan Agriculture University in 2022. He is now a Master's student in Dalian Maritime University. His research interest is integration of communication, sensing and control in the Industrial Internet of Things.

Ling Lyu received her BS in Telecommunication Engineering from Jinlin University, Changchun, China, in 2013, and the PhD in Control Theory and Control Engineering from Shanghai Jiao Tong University, Shanghai, China, in 2019. She joined Dalian Maritime University, Dalian, China, in 2019, where

she is currently an Associate Professor with the School of Information Science and Technology. She was a Visiting Student with the University of Waterloo, Waterloo, ON, Canada from September 2017 to September 2018. Her current research interests include wireless sensor and actuator network and application in industrial automation, the joint design of communication and control in industrial cyber-physical systems, estimation and control over lossy wireless networks, machine type communication enabled reliable transmission in the fifth generation network, resource allocation, and energy efficiency.

Yanpeng Dai received his BE from Shandong Normal University, Jinan, China, in 2014, and the PhD from Xidian University, Xi'an, China, in 2020. He is currently an Assistant Professor with the School of Information Science and Technology, Dalian Maritime University, Dalian, China. He was a Visiting Student at the University of Waterloo, Waterloo, ON, Canada. His research interests include resource management and interference coordination for heterogeneous wireless networks.

1 Introduction

With the rapid deployment of information and communications technologies, many existing works have pointed out that ubiquitous sensing over Internet of Things (IoT) plays an increasingly important role in industrial automation (Gao et al., 2019; Yang et al., 2019; Lyu et al., 2019). In industrial IoT system, a large number of sensors are deployed to in the field to monitor the system operation state. The collected sensing information then delivered to the remote controller for making decision. Due to the harsh industrial wireless environment and limited transmit power of sensors, it is very difficult to directly transmit the sensing information to the remote controller. Huang et al. (2023) supported that unmanned aerial vehicles (UAVs) can be introduced to take advantage of its flexible deployment, wide area coverage, and line-of-sight communication for data collection and transmission. Zhang et al. (2022) supported the possibility of introducing highly durable, autonomous and safe AGVs that can be moved to different areas for data collection. However, the mobility of UAVs and automated guided vehicles (AGVs) make it challenging to timely obtain the accurate channel condition, especially in the indoor scenario. Inaccurate channel conditions affect data transmission and makes it difficult to meet the high performance of industrial IoT.

In recent years, industrial IoT requires not only high-quality transmission capacity but also high-precision sensing ability. Liu et al. (2022) supported the concept of integrated sensing and communication (ISAC), which aims to integrate sensing and communication to share the same spectrum and infrastructure, has received increasing attention from academia and industry. Wu et al. (2022) supported communication-sensing integrated systems can further benefit from mutual assistance, such as sensing-assisted communication and communication-assisted sensing. However, how to improve the sensing-and-communication tightness and reduce the mutual interference is a problem needed to be solved. Meng et al. (2023) supported to consider embedding sensing functions on the existing communication signals so that the sensing functions are triggered periodically to maximise the system reachable rate. However, periodic sensing and communication perform alternately in the time domain, which does not increase the spectrum utilisation and has limited improvement for system performance.

In order to support high data speeds and large-scale connectivity on limited spectrum resources, it is critical to investigate multiple access technologies for next-generation wireless systems. Non-orthogonal multiple access (NOMA) is a multiple access technique that provides an additional domain to separate users on the same resource block in order to detect superimposed user information using successive interference cancellation (SIC). Krishnamoorthy and Schober (2021) supported that NOMA has the potential to improve the spectral efficiency and data rates of 5th-generation (5G) and later mobile communication systems. Du et al. (2017) supported that large-scale connectivity can be supported by non-orthogonal resource allocation among devices using limited resources. Due to the strong superposition of NOMA, the combination of NOMA and ISAC can solve the coupling problem of sensing and communication signals, and further realise the integration of communication and sensing. Wang et al. (2022) supported the first framework for the application of NOMA technique in ISAC, where the transmitter sends superimposed signals for both communication and sensing, and uses SIC technique to mitigate inter-user interference at the communication receiver, but how to design a compliant sensing beam is very important to achieve interference cancellation. Memisoglu et al. (2023) supported classical NOMA communication, but using echoes of NOMA signals for radar sensing. All these works consider beamforming communications, and as in most power domain NOMA works, assume that the communicating users has perfect channel knowledge. In summary, the combination of NOMA and ISAC can eliminate the interference of sensing to communication using SIC, but the degree of interference elimination and the achievable data rate are closely related to the channel condition between transceivers.

In the UAV-assisted industrial IoT systems, the mobility of UAVs and AGVs make it challenging to timely obtain the accurate channel condition. In order to address this issue, this paper investigates a sensing-communication-control integrated architecture for UAV-assisted industrial IoT systems. To achieve high-quality transmission performance with low energy consumption, the ratio of transmission rate to power consumption is used to evaluate the system efficiency. We aim to maximise system efficiency by jointly optimising the communication power and beamforming vectors. The contributions of this paper are summarised as below.

- We propose a sensing-communication-control integrated architecture for UAV-assisted industrial IoT systems, where the sensing-based motion control is performed to adjust the location of UAV to improve the channel condition and transmission rate.
- The designed integration of sensing, communication and control (ISCC) scheme has superiorities in improving the overall performance of UAV-assisted industrial IoT systems, since it enhances data rate by suppressing interference.
- A dual-layer penalty based successive convex approximation algorithm is designed to effectively solve the non-convex problem.

2 System model

The considered UAV-assisted industrial IoT systems is shown as Figure 1, where sensors deployed in the filed take charge of monitoring system state. Moreover, AGV take charge of collecting sensing information and then delivering to the UAV. As we all known that the data transmission rate heavily depends on the channel condition. However, the mobility of UAVs and AGVs make it challenging to timely obtain the accurate channel condition, especially in the indoor scenario. In order to address this issue, the emerging ISAC technology is introduced to achieve the location sensing and data transmission simultaneously on the same frequency band. With the ISAC technology, Hua et al. (2023) supported that AP with uniform linear array (ULA) can use beamforming techniques to achieve localisation of UAVs and AGVs. In this case, UAV will suffer the co-frequency interference from the sensing signals transmitted by AP. In this work, the power-domain NOMA technology is employed to suppress interference. Assuming that the AP is positioned at the origin of the coordinate system, the positions of the AGV and UAV are denoted as $\mathbf{Q}_1(q_{x1}, q_{y1}, q_{z1})$ and $\mathbf{Q}_2(q_{x2}, q_{y2}, q_{z2})$, respectively. The communication, sensing, and control models, and control trigger scheme are described as below.

Figure 1 Integration of sensing, communication, and control for UAV-assisted data transmission in industrial IoT systems (see online version for colours)

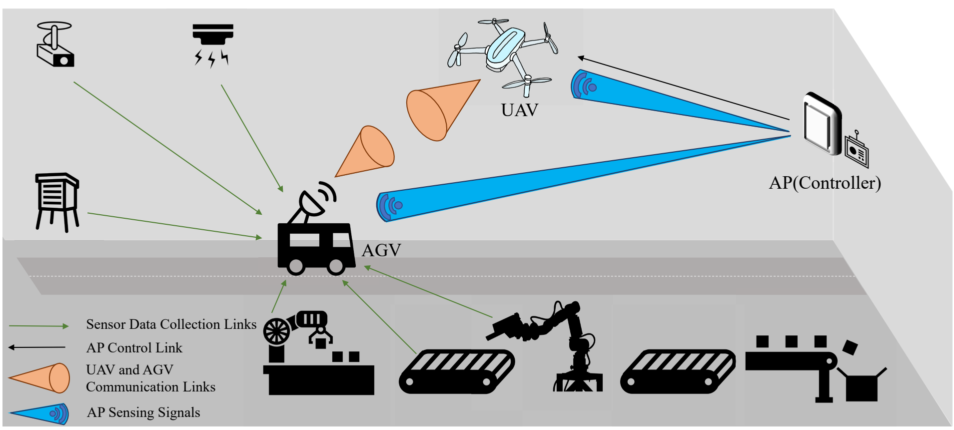

2.1 Communication model

In the considered system, the AP is equipped with an N-antenna ULA. Both UAV and AGV are equipped with horn antennas. In this subsequent subsection, the signal model and channel model are introduced.

1 *Signal model*: The signal received by UAV can be expressed as

$$y_u = hs_a + \mathbf{h}_s\mathbf{x} + \omega, \tag{1}$$

where $s_a \in \mathbb{C}$ is the communication signal from AGV, $\mathbf{x} \in \mathbb{C}^{N\times1}$ is the sensing signal from the AP, $h \in \mathbb{C}$ and $\mathbf{h}_s \in \mathbb{C}^{N\times1}$ are respectively the flat fading wireless channel between AGV and UAV and between AP and UAV, $w \in \mathbb{C}$ is additive noise with zero-mean and variance N_0, i.e., $w \sim \mathcal{CN}(0, N_0)$. In NOMA based wireless transmission, the SIC technology is general used eliminate the signal of weak users from the received signal of strong users to improve the signal to interference plus noise ratio. Depending on the received power, the achieved data rate with SIC technology could be given by

$$R = \begin{cases} \log_2(1 + \frac{|h|^2 P_c}{N_0}), & \text{when } \Delta < P_c < P_s, \\ \log_2(1 + \frac{|h|^2 P_c}{P_s + N_0}), & \text{when } \Delta < P_s < P_c \text{ or } P < \Delta, \end{cases} \tag{2}$$

where Δ denotes the decoding interval, P_c denotes the transmit power of the communication signal, and P_s represents the received power of the sensing signal at the UAV. When the condition for SIC is satisfied, either the sensing signal or the communication signal can be eliminated, as indicated in equation (2). However, if the SIC condition is not met, the sensing signal will still impact the data rate as interference.

2 *Channel model*: Chang et al. (2022) supported that the flat fading wireless channel includes multipath fading, path-loss and misalignment fading. Then, the channel gain h could be expressed as

$$h = h_p h_f h_m. \tag{3}$$

- **Path loss**: The path loss could be described with the free-space propagation model, which is expressed as

$$h_p = \frac{\sqrt{G_t G_r}\lambda}{4\pi d}, \tag{4}$$

where G_t and G_r are the transmit and receive signal gains, respectively. $\lambda = \frac{f}{c}$ is the signal wavelength, where c is the speed of light, and f is the occupied frequency band. d is the distance between transceivers.

- **Multipath fading**: Boulogeorgos et al. (2019) supported the multipath fading is usually described with the Rayleigh distribution, where the probability distribution function is given by

$$f_{h_f} = \frac{2}{\hat{h}_f^2 \Gamma(1)} \cdot x \cdot e^{-\frac{x^2}{\hat{h}_f^2}}, \tag{5}$$

where $\hat{h}_f$ is the fading channel with the root mean square value $\alpha = 2$.

- **Misalignment fading**: We assume that the transmitting beam of UAV covers a region S with radius R. Meanwhile, the radius of the area covered by the AGV beam is r and the distance is d, where $0 \leq R \leq R_m$ and R_m are the maximum radius of the beam at distance d. In addition, l is the misalignment error between the beam centre O_{AGV} of AGV and the beam centre O_{UAV} of UAV. As shown in Figure 2, the misalignment cases are classified into three types according to the relationship between l and R. Then, the misalignment fading can be expressed as

$$h_m = P_0 e^{-\frac{2l^2}{R_e^2} e_\theta}, \tag{6}$$

which indicates that misalignment fading is the received power of UAV at distance d in the area S. Then, the beam-width is represented by R_e. e_θ is the error of the horn antenna. In this paper, the misalignment errors for the first stage consider only the position errors in the x and y axis directions, denoted by x_1 and x_2, i.e., $l = \sqrt{x_1^2 + x_2^2}$. In addition, when $l = 0$ the received power can be represented as P_0, would could be obtained by

$$P_0 = erf(\epsilon)^2, \tag{7}$$

where $\epsilon = (\sqrt{\pi}r)/(\sqrt{2}R_m)$. and $erf(\cdot)$ is Gauss error function. Then, R_e can be expressed as

$$R_e^2 = R_m^2 \frac{\sqrt{\pi} erf(\epsilon)}{2\varepsilon e^{-\epsilon^2}}. \tag{8}$$

Figure 2 Misalignment error l and three conditions (see online version for colours)

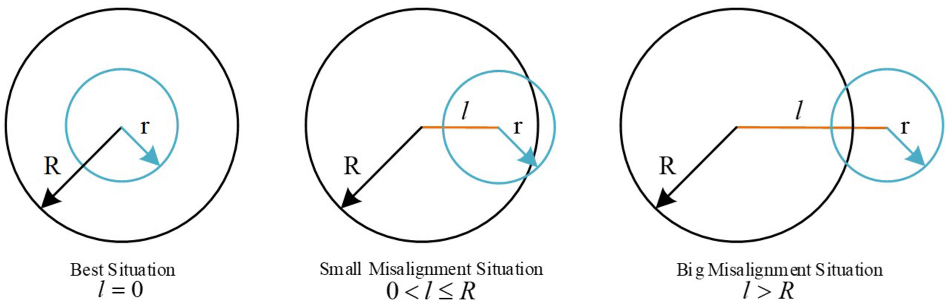

2.2 *Sensing model*

The key indicator of the sensing function is the covariance matrix of the sensing beam distribution determined by the transmit signal. The covariance matrix is given by

$$\mathbf{R}_w = \mathbb{E}\left[\mathbf{x}\mathbf{x}^H\right] = \sum_{i=1}^{M} \mathbf{w}_i \mathbf{w}_i^H, \tag{9}$$

where $\mathbf{w}_i$ is the transmitting beamformer of the sensing signal, M is the number of sensing targets. Then, AP transmits the sensing signal power as

$$P_t = \text{Tr}(\mathbf{R}_w). \tag{10}$$

Then, the sensing beampattern in the direction φ_m is given by

$$H(\varphi_m) = \mathbf{a}^{\mathbf{H}}(\varphi_m)\mathbf{R}_w\mathbf{a}(\varphi_m), \tag{11}$$

where $\mathbf{a}(\varphi_m) = [1, e^{j\frac{2\pi}{\lambda}d\sin(\varphi_m)}, ..., e^{j\frac{2\pi}{\lambda}d(N-1)\sin(\varphi_m)}]^T$ denotes the steering vector when ULA is used as the antenna employment at AP. In practice, Wang et al. (2022) supported that the desired sensing beampattern is designed according to the sensing requirements. For example, if the sensing system has no information about target and works in the detecting mode, an isotropic beampattern is desired, i.e., the power is uniformly distributed among all directions. However, when the sensing system has prior information of targets and works in the tracking mode, the beampattern is expected to have the dominant peaks in the target directions. Then, according to (Wu et al., 2018), the sensing channel h_s is expressed as

$$\mathbf{h}_s = \sqrt{\frac{\beta}{H^2 + \|Z_m - Z_a\|}}\mathbf{a}(\varphi_m), \tag{12}$$

where β is channel gain value at a distance of 1m from the AP. H indicates the height of the AGV or UAV. Thus, the power of AP sensing UAV is expressed as

$$P_s = \left|\mathbf{h}_s^H \mathbf{w}_2\right|^2 = \left|\mathbf{h}_s^H \mathbf{W}_2 \mathbf{h}_s\right|. \tag{13}$$

In this paper, only the beam assignment in the horizontal direction is considered. The AP lies at the origin of the coordinate axis and do not consider the vertical direction. Based on the position information of the AGV and UAV, the horizontal angle is

$$\varphi_m = \arcsin \frac{q_{xm}}{\sqrt{q_{xm}^2 + q_{ym}^2}}, \tag{14}$$

where q_{xm} and q_{ym} are the position of the sensing target in the x-axis and y-axis direction, respectively.

2.3 Control model

1 *UAV Motion control model*: Dai et al. (2022) supported that the discrete-time control model is obtained as

$$\mathbf{x}_{k+1} = \mathbf{A}_d x_k + \mathbf{B}_d u_k + \mathbf{w}_k, \tag{15}$$

where $\mathbf{A}_d$ and $\mathbf{B}_d$ are the system parameter matrices in the discrete-time model. u_k is the motion control input, and $\mathbf{w}_k$ is the perturbation caused by additive gaussian white noise with zero mean and variance W.
Wang et al. (2012) , Li et al. (2016) and Wu et al. (2020) all supported that the sampled state at AP is perfect at each time indicator k, then $\mathbf{y}_k = \mathbf{x}_k$. According to the equation (15), the controller can calculate the control input at the AP as

$$u_k = \mathbf{K}\mathbf{y}_k, \tag{16}$$

where $\mathbf{K}$ is the control gain. Furthermore, Zeng et al. (2019) supported, for a rotorcraft UAV with speed V_k, the propulsion power consumption can be modelled as

$$P_{f,k}(V_k) = P_b\left(1 + \frac{3V_k^2}{U_{\text{tip}}^2}\right) + \frac{P_i v_o}{V_k} + \frac{1}{2} d_o \rho s w_o V_k^3, \tag{17}$$

where U_{tip} is the rotor blade tip speed, v_o is the average rotor induced speed, d_o is the body drag ratio, P_b and P_i are the blade profile power and induced power respectively, ρ, s and w_o are the air density, rotor solidity and blade angular velocity respectively.

Then, the UAV velocity in the discrete domain is calculated by the following equation

$$V_k = \frac{|\mathbf{Q}_{2,k} - \mathbf{Q}_{2,k-1}|}{\Delta_0}. \tag{18}$$

2 *Horn antenna angle control model*: The distance and relative angle between UAV and AGV can be obtained through sensing measurements. The direction of the horn antenna on the UAV can be represented by the pitch angle θ and azimuth angle ϕ. As the UAV and AGV remain in relative motion, this paper simplified the antenna control model by considering that the azimuth between them remains optimally constant. Based on the knowledge of trigonometric functions, the angle of the direction at which the horn antenna points towards the device can be calculated as θ_d, where

$$\theta_d = \tan^{-1}\left(\frac{q_{x1} - q_{x2}}{\sqrt{(q_{x1} - q_{x2})^2 + (q_{y1} - q_{y2})^2}}\right). \tag{19}$$

Then, the error of the current horn antenna pointing direction is $e_{\theta,k} = \theta_k - \theta_{d,k}$, θ_k is the UAV at the kth moment antenna pointing direction angle, which can be obtained through the UAV's built-in sensor. We can use a controller to control the direction of the horn antenna, the control output can be expressed as

$$z_k = K_a \theta_k, \tag{20}$$

where K_a is the control gain. The discrete-time control model for horn antenna angle control of UAV is

$$\theta_{k+1} = A_a \theta_k + B_a z_k + w_k, \tag{21}$$

where A_a and B_a are system parameter matrix, respectively. w_k is disturbance.

2.4 Control trigger scheme

As the location of UAV heavily impact the transmission rate, it is necessary to adjust the UAV's location based on the channel condition and transmission requirement. However, the location changing will cause energy consumption. Therefore, it is necessary to investigate the control trigger scheme, which aims to meet the transmission rate requirements between AGV and UAV as well as reduce the holistic energy consumption. AGV delivers the collected sensing information to UAV. At the same time, AP transmits the sensing signals to obtain the location of AGV and UAV. Then, AP calculates the misalignment, which is a key index to trigger the motion control of UAV. The control trigger factor is given by

$$\varepsilon_k = \begin{cases} 1, & \text{when } l_{k+1} > R, \\ 0, & \text{when } l_{k+1} \leq R. \end{cases} \tag{22}$$

As shown in Figure 3, AP makes a judgement based on the misalignment error l in relation to the beam radius R of UAV. When $l > R$, the AP will issue UAV motion control and antenna angle control commands, otherwise it will only issue antenna angle control commands.

Figure 3 Control trigger scheme

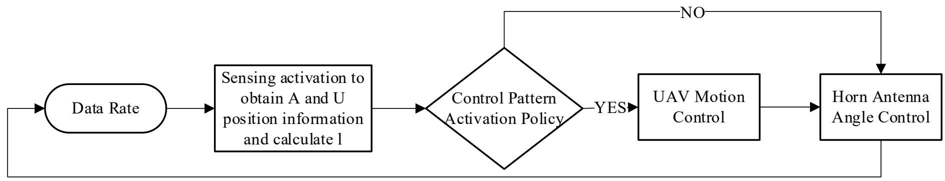

3 Problem formulation and proposed solution

3.1 Problem formulation

Based on the above discussion, the sensing, communication and control are jointly designed to maximise the ratio of the total amount of data rata to the total power consumption while meeting AGV communication power and radar specific requirements. The constrained optimisation problem is formulated as

$$\begin{aligned} \mathcal{P}_0 : \max_{P_c, \mathbf{w}_k} \quad & \frac{R}{P_c + P_t + \varepsilon P_f} \\ \text{s.t.} \quad & \text{C1} : \varepsilon \in \{0, 1\}, \\ & \text{C2} : |H(\varphi_1) - H(\varphi_2)\ | \leq P_d, \\ & \text{C3} : H(\varphi_m) \geq H(\psi), \forall m \in M, \\ & \text{C4} : P_t \leq P_l, \\ & \text{C5} : \mathbf{R}_w \succeq 0, \\ & \text{C6} : 0 < |h|^2 P_c < P_s, \end{aligned}$$

where C1 denotes the 0-1 constraint on the control activation factor. C2 and C3 are the constraints that ensure the similar induced power levels in different target directions, where P_d is the proposed minimum power difference and $\psi \in [-90°, 90°]$ is the sensing range. C4 is the maximum transmit power constraint, where P_l denotes sensing power budget. C6 is the constraints of the SIC conditions. It is challenging to obtain the globally optimal solution of the formulated problem $\mathcal{P}_0$ due to the quadratic form of the covariance matrix makes the constraints C2-C6 non-convex. In order to effectively solve the problem, we design a Double-Layer Penalty-Based Algorithm.

3.2 Double-layer penalty-based algorithm

Define the auxiliary variables $\mathbf{W}_k = \mathbf{w}_k \mathbf{w}_k^H, \forall k \in \mathcal{K}$, where $\mathbf{W}_k \succeq 0$ and $\text{rank}(\mathbf{W}_k) = 1$. Then, $\mathcal{P}_0$ can be reformulated as

$$\begin{aligned} \mathcal{P}_1 : \max_{P_c, \mathbf{W}_k} \quad & \frac{R}{P_c + P_t + \varepsilon P_f} \\ \text{s.t.} \quad & \text{C1} - \text{C6}, \\ & \text{C7} : \mathbf{W}_k \succeq 0, \mathbf{W}_k = \mathbf{W}_k^H, \forall k \in \mathcal{K}, \\ & \text{C8} : \text{rank}(\mathbf{W}_k) = 1. \end{aligned}$$

Semi definite relaxation (SDR) method is regarded as an effective method deal with the no-convex rank-one constraint C8. Luo et al. (2010) supported that the general-rank solution obtained from the SDR could be reconstructed as a rank-one solution using an eigenvalue decomposition or Gaussian randomisation method. However, this may lead to a large performance loss and do not guarantee the feasibility of the reconstructed matrix. To avoid these drawbacks, the rank one constraint is transformed into a penalty term in the objective function and then solve the problem by SCA. The rank-one constraints are equivalent to

$$\|\mathbf{W}_k\|_* - \|\mathbf{W}_k\|_2 = 0, k \in \mathcal{K}, \tag{23}$$

where $\|\cdot\|_*$ is the nuclear norm, i.e., the sum of singular values of the matrix. $\|\cdot\|_2$ is the spectral norm, i.e., the largest singular values of the matrix. Thus, if the matrix $\mathbf{W}_k$ is a rank-one matrix, the equation (23) holds. Otherwise, if $\mathbf{W}_k$ is semidefinite, the sum of singular values is larger than the largest singular value, i.e., $\|\mathbf{W}_k\|_* - \|\mathbf{W}_k\|_2 > 0$. In order to obtain a rank-one matrix, a penalty term based on the equation (23) is introduced to the objective function, yielding that

$$\begin{aligned}
\mathcal{P}_{1.1}: \max_{P_c, \mathbf{W}_k} \quad & \frac{R}{P_c + P_t + \varepsilon P_f} - \frac{1}{\eta}\left(\|\mathbf{W}_k\|_* - \|\mathbf{W}_k\|_2\right) \\
\text{s.t.} \quad & \text{C1} - \text{C6}, \\
& \text{C7}: \mathbf{W}_k \succeq 0, \mathbf{W}_k = \mathbf{W}_k^H, \forall k \in \mathcal{K},
\end{aligned}$$

where η is the penalty factor and the rank of $\mathbf{W}_k$ is closer to 1 only when it tends to 0, i.e., $\frac{1}{\eta}$ tends to ∞. In this case, the main non-convexity of $\mathcal{P}_{1.1}$ comes from the second term of the penalty term, which is replaced with its first-order Taylor expansion at the point $\mathbf{W}_k^n$. The original equation could be transformed as

$$-\|\mathbf{W}_k\|_2 \leq \tilde{\mathbf{W}}_k^n \triangleq -\|\mathbf{W}_k^n\|_2 - \mathrm{Tr}\left[\mathbf{v}_{\max,k}^n (\mathbf{v}_{\max,k}^n)^H (\mathbf{W}_k - \mathbf{W}_k^n)\right], \tag{24}$$

where $\mathbf{v}_{\max,k}^n$ is the eigenvector corresponding to the largest eigenvalue of $\mathbf{W}_k^n$. Then, the problem $\mathcal{P}_{1.2}$ can be approximated by the following problem

$$\begin{aligned}
\mathcal{P}_{1.2}: \max_{P_c, \mathbf{W}_k} \quad & \frac{R}{P_c + P_t + \varepsilon P_f} - \frac{1}{\eta}\left(\|\mathbf{W}_k\|_* + \|\tilde{\mathbf{W}}_k^n\|_2\right) \\
\text{s.t.} \quad & \text{C1} - \text{C7}.
\end{aligned}$$

The problem $\mathcal{P}_{1.2}$ can be solved by logarithmising the objective function. As we mentioned above that the η value can only be closer to the rank-one constraint if the penalty term is sufficiently small. However, another problem is that the value of the objective function tends to infinity. As a result, the value fitting the rule is hard to obtain. A penalty factor ϵ is involved to deal with this problem. Then, the value of $\eta = \epsilon\eta, 0 < \epsilon < 1$ is sufficiently small by letting the value of ϵ be large. The overall suboptimal solution is obtained, if the penalty term is small enough, i.e., $\|\mathbf{W}_k\|_* - \|\mathbf{W}_k\|_2 \leq \varepsilon_2$. The overall algorithm for the problem is summarised in Algorithm 1.

Algorithm 1 Proposed Double-Layer Penalty-Based Algorithm.

Input: φ_m, $\mathcal{M}$, η;
Output: P_c, $\mathbf{W}_k$;
Initialization: feasible $\mathbf{W}_k^0$, ϵ, ε_1, ε_2;
repeat
  $n \longrightarrow 0$
  repeat
    Solve $\mathcal{P}_{1.2}$ according to $\mathbf{W}_k^n$;
    Update $\mathbf{W}_k^{n+1}$ based on $\mathbf{W}_k^n$;
    $n \longleftarrow n+1$;
  until $\iota = \frac{|f_n - f_{n-1}|}{f_{n-1}} \leq \varepsilon_1$
  $\mathbf{W}_k^0 \longleftarrow \mathbf{W}_k^n$;
  $\eta \leftarrow \epsilon\eta$;
until $\|\mathbf{W}_k\|_* - \|\mathbf{W}_k\|_2 \leq \varepsilon_2$;

4 Simulation results

In this section, numerical results are provided to demonstrate the feasibility of the proposed integrated the sensing-communication-control integrated architecture for UAV-assisted industrial IoT systems. AP is equipped with $N = 4$ antennas that tracks both UAV and AGV based on location information. The power budget for communication and radar are 27dBm and 30dBm, respectively. The power of the noise $\sigma_n^2 = -110\text{dBm}$, and the sensing power interval $P_d = 5$. The beam radii of UAV and AGV at distance d are $R = 1$ and $r = 0.5$ respectively. For UAV power consumption, $U_{tip} = 120$ is the rotor blade tip speed, $v_o = 4.03$ is the average rotor induced speed, $d_o = 0.6$ is the body drag ratio, $P_b = 79.9$ and $P_i = 88.6$ are the blade profile power and induced power respectively, $\rho = 1.225$, $s = 0.05$ and $w_o = 0.503$ are the air density, rotor solidity and blade angular velocity respectively. The initial values of the simulation are $\epsilon = 0.4$, $\varepsilon_1 = 0.1$, $\varepsilon_2 = 10^{-6}$. Initial positions with $\mathbf{Q}_1(20, 34.6, 10)$ and $\mathbf{Q}_2(-20, 34.6, 0)$.

Figure 4 shows the convergence of the proposed double-Layer penalty-based algorithm. It can be seen that for a given penalty factor, the objective value converges to a stable value and the penalty term converges to almost zero after several iterations, although the number of antennas of AP is different. However, the increase in the number of antennas leads to an increase in the fluctuation of the objective value and the penalty term value with the number of iterations. Moreover, the sensing power increases rapidly when $N = 8$, which further leads to an increase in the denominator of the objective function and makes the objective value smaller.

Figure 5 shows the comparison between the communication rate and the misalignment error for the case that the SIC condition is satisfied or not. It can be seen that the communication rate is greater when the SIC condition is satisfied, no matter what the value of the misalignment error is. Therefore, the UAV motion control and the antenna angle control involved in the proposed ISCC scheme could achieve high data transmission rate with low energy cost. Therefore, the adjustment of misalignment error can improve the communication rate, which further verifies the necessary of the integration of sensing and communication.

Figure 4 Comparison of objective function values and penalty term values with different number of sensing antennas (see online version for colours)

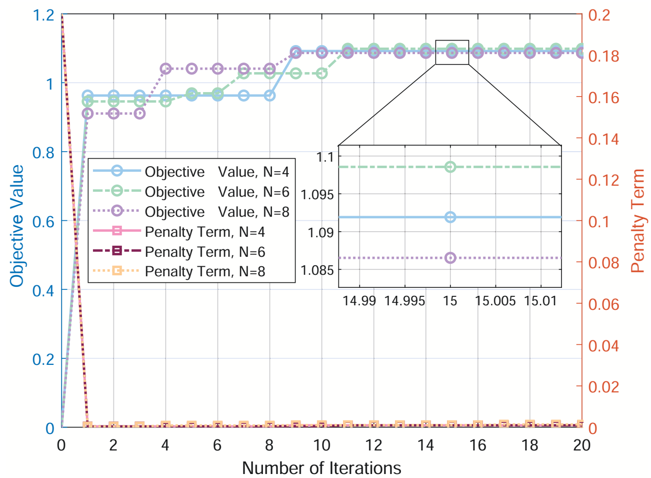

Figure 5 Comparison of the transmission rate with misalignment error under different NOMA conditions (see online version for colours)

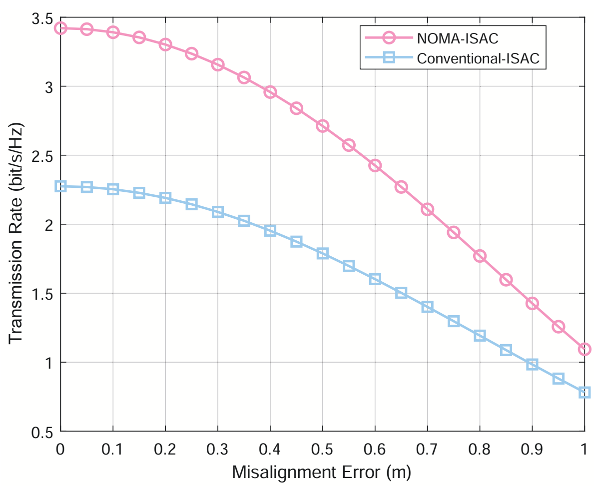

Figure 6 shows the transmission rate variation with different power budget under different levels of misalignment errors. It can be seen that the transmission increases in all cases with the growth of transmit power. Therefore, the proposed method in this paper is able to appropriate perform control operations to improve the transmission rate with limited power budget.

Figure 7 shows the beampattern calculated from the beamforming vectors corresponding to the proposed ISCC scheme at the transmission rate of 3.42 bit/s/Hz. It can be seen that the solved beamforming vector reaches the peak in the horizontal direction of the sensing target, i.e., –30° and 30°. Moreover, the power is very small in the direction that does not need to be sensed, which ensures the sensing accuracy in the target direction with limited energy budget.

Figure 6 Comparison of the variation of the transmission rate with power limit under different misalignment conditions (see online version for colours)

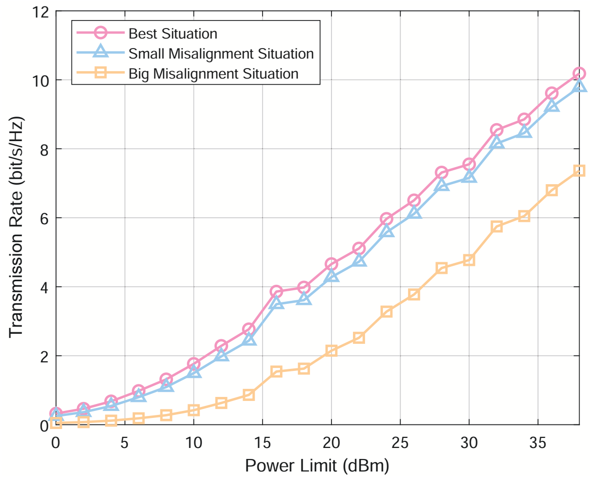

Figure 7 Beampattern of AP when $N = 4$ (see online version for colours)

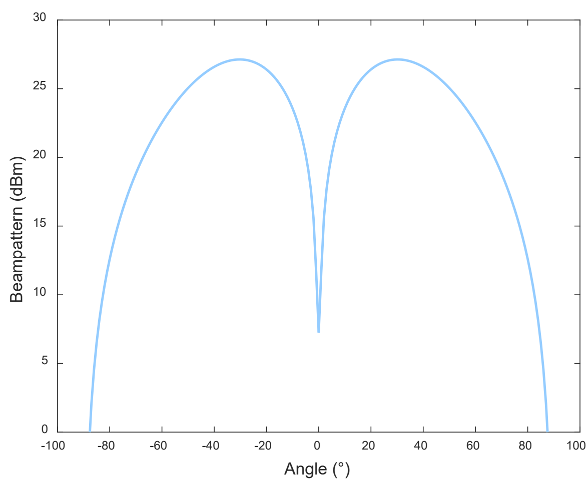

5 Conclusion

In this paper, we proposed a sensing-communication-control integrated architecture for UAV-assisted industrial IoT systems, where the sensing-based motion control is performed to adjust the location of UAV to improve the channel condition and transmission rate. The investigated ISCC scheme could reduce the interference of sensing signals to communication signals by jointly designing the transmit power and beamformers. Moreover, the formulated non-convex constrained optimisation problem is effectively solved with the designed double-layer penalty-based algorithm. The numerical results indicated that a significant performance gain can be achieved by the NOMA assisted ISCC scheme than the conventional ISAC system.

Acknowledgement

This work is supported in part by National Natural Science Foundation of China under 62002042 and 62101089, in part by China Postdoctoral Science Foundation under 2021M690022 and 2021M700655, in part by Doctoral Research Startup Funds of Liaoning Province under Grant 2023-BS-068.

References

Boulogeorgos, A.A., Papasotiriou, E.N. and Alexiou, A. (2019) 'Analytical performance assessment of the wireless systems', *IEEE Access*, Vol. 7, pp.11436–11453.

Chang, B., Tang, W., Yan, X., Tong, X. and Chen, Z. (2022) 'Integrated scheduling of sensing, communication, and control for mmwave/thz communications in cellular connected UAV networks', *IEEE Journal on Selected Areas in Communications*, Vol. 40, No. 7, pp.2103–2113.

Cheng, N., Lyu, F., Quan, W., Zhou, C., He, H., Shi, W. and Shen, X. (2019) 'Space/aerial-assisted computing offloading for IoT applications: a learning-based approach', *IEEE Journal on Selected Areas in Communications*, Vol. 37, No. 5, pp.1117–1129.

Dai, Y., Lin, B., Che, Y. and Lyu, L. (2022) 'UAV-assisted data offloading for smart container in offshore maritime communications', *China Communications*, Vol. 19, No. 1, pp.153–165.

Du, Y., Dong, B., Chen, Z., Wang, X., Liu, Z., Gao, P., Li, S. (2017) 'Efficient multi-user detection for uplink grant-free NOMA: prior-information aided adaptive compressive sensing perspective', *IEEE Journal on Selected Areas in Communications*, Vol. 35, No. 12, pp.2812–2828.

Gao, J., Zhuang, W., Li, M., Shen, X. and Li, X. (2019) 'MAC for Machine-Type Communications in Industrial IoT–Part I: Protocol design and analysis', *IEEE Internet of Things Journal*, Vol. 8, No. 12, pp.9945–9957.

Hua, H., Xu, J. and Han, T.X. (2023) 'Optimal transmit beamforming for integrated sensing and communication', *IEEE Transactions on Vehicular Technology*, Vol. 72, No. 8, pp.10588–10603.

Huang, X. and Fu, X. (2023) 'Fresh data collection for UAV-assisted IoT based on aerial collaborative relay', *IEEE Sensors Journal*, Vol. 23, No. 8, pp.8810–8825.

Krishnamoorthy, A. and Schober, R. (2021) 'Uplink and Downlink MIMO-NOMA with simultaneous triangularization', *IEEE Transactions on Wireless Communications*, Vol. 20, No. 6, pp.3381–3396.

Li, Q., Yang, S., Pan, J., Xu, B. and Li, H. (2016) 'Robust control for a networked directdrive linear motion control system: design and experiments', *Information Sciences*, Vol. 370, pp.725–742.

Liu, F., Cui, Y., Masouros, C., Xu, J., Han, T.X., Eldar, Y. and Buzzi, S. (2022) 'Integrated sensing and communications: toward dual-functional wireless networks for 6G and beyond', *IEEE Journal on Selected Areas in Communications*, Vol. 40, No. 6, pp.1728–1767.

Luo, Z., Ma, W., So, A.M., Ye, Y. and Zhang, S. (2010) 'Semidefinite relaxation of quadratic optimization problems', *IEEE Signal Processing Magazine*, Vol. 27, No. 3, pp.20–34.

Lyu, L., Zhao, L., Dai, Y., Cheng, N., Chen, C., Guan, X. and Shen, X. (2023) 'Adaptive edge sensing for industrial IoT systems: estimation task offloading and sensor scheduling', *IEEE Internet of Things Journal*, Vol. 10, No. 1, pp.391–402.

Memisoglu, E., Türkmen, H., Ozbakis, B.A. and Arslan, H. (2023) 'CSI-Based NOMA for Integrated Sensing and Communication', *IEEE Communications Letters*, Vol. 12, No. 6, pp.1086–1090.

Meng, K., Wu, Q., Ma, S., Chen, W., Wang, K. and Li, J. (2023) 'Throughput maximization for UAV-enabled integrated periodic sensing and communication', *IEEE Transactions on Wireless Communications*, Vol. 22, No. 1, pp.671–687.

Wang, J. and Ming, X. (2012) 'Integrated optimal formation control of multiple unmanned aerial vehicles', *IEEE Transactions on Control Systems Technology*, Vol. 21, No. 5, pp.1731–1744.

Wang, Z., Liu, Y., Mu, X., Ding, Z. and Dobre, O. (2022) 'NOMA empowered integrated sensing and communication', *IEEE Communications Letters*, Vol. 26, No. 3, pp.677–681.

Wang, Z., Liu, Y., Mu, X. and Ding, Z. (2022) 'NOMA inspired interference cancellation for integrated sensing and communication' *ICC 2022: IEEE International Conference on Communications*, Foshan, China, pp.3154–3159.

Wu, Q., Xu, J. and Zhang, R. (2018) 'Capacity characterization of UAV-enabled two-user broadcast channel', *IEEE Journal on Selected Areas in Communications*, Vol. 36, No. 9, pp.1955–1971.

Wu, X., She, J., Yu, L., Dong, H. and Zhang, W. (2020) 'Contour tracking control of networked motion control system using improved equivalent-input-disturbance approach', *IEEE Transactions on Industrial Electronics*, Vol. 68, No. 6, pp.5155–5165.

Wu, Q., Xu, J., Zeng, Y., Ng, D. W. K., Al-Dhahir, N., Schober, R., Swindlehurst, A. L. (2021) 'A Comprehensive Overview on 5G-and-beyond networks With UAVs: from communications to sensing and intelligence', *IEEE Journal on Selected Areas in Communications*, Vol. 39, No. 10, pp.2912–2945.

Yang, Z., Wang, R., Wu, D., Wang, H., Song, H. and Ma, X. (2019) 'Local trajectory privacy protection in 5G enabled industrial intelligent logistics', *IEEE Transactions on Industrial Informatics*, Vol. 18, No. 4, pp.2868–2876.

Zeng, Y., Xu, J. and Zhang, R. (2019) 'Energy minimization for wireless communication with rotary-wing UAV', *IEEE Transactions on Wireless Communications*, Vol. 18, No. 4, pp.2329–2345.

Zhang, Y., Liu, Y., Sun, G., Li, J. and Wang, A. (2022) 'Multi-objective optimization for joint UAV-AGV collaborative beamforming' *2022 IEEE International Conference on Systems, Man, and Cybernetics*, Prague, Czech Republic, pp.150–157.